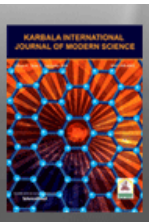

Karbala International Journal of Modern Science

Volume 8 | Issue 3 Article 5

Applicability limits of the end face fiber-optic gas concentration sensor, based on Fabry-Perot interferometer

S.M.R.H. Hussein
University of Karbala, Karbala, 56001, Iraq,

A.Zh. Sakhabutdinov
Kazan National Research Technical University named after A.N. Tupolev-KAI, 10, K. Marx str., 420011, Kazan, Russian Federation, azhsakhabutdinov@kai.ru

O.G. Morozov
Kazan National Research Technical University named after A.N. Tupolev-KAI, 10, K. Marx str., 420011, Kazan, Russian Federation

V.I. Anfinogentov
Kazan National Research Technical University named after A.N. Tupolev-KAI, 10, K. Marx str., 420011, Kazan, Russian Federation

J.A. Tunakova
Kazan National Research Technical University named after A.N. Tupolev-KAI, 10, K. Marx str., 420011, Kazan, Russian Federation

See next page for additional authors

Applicability limits of the end face fiber-optic gas concentration sensor, based on Fabry-Perot interferometer

Abstract

The mathematical model of the fiber-optic sensor for gas concentration analysis is under study. The sensor is imple-mented as Fabry-Perot interferometer at the end face of the optical fiber by applying a thin polymer film, which permit-tivity depends on the tested gas concentration. It is shown, that a change in the properties of the optical fiber or the at-mosphere permittivity leads mainly to the spectrum contrast changing and does not change the period and the wave-length shift of its comb. The influence of the polymer film thickness, the environment temperature and humidity on the Fabry-Perot spectrum is analyzed. The necessity of using the temperature and humidity compensation sensors is shown. The method, which determines the permittivity in narrow and wide ranges basing on the comb period and the wave-length shift of Fabry-Perot reflection spectrum, is developed. The relative error of measuring the polymer film permit-tivity depending on the film thickness for three wavelength ranges (810–890, 1270–1350, and 1510–1590 nm) is esti-mated. The real achievable relative error in determining the polymer film permittivity is in 0.3–1% FSI, depending on the conditions of the experiment. The mathematical methods and practical recommendations are proposed.

Keywords

Fabry-Perot interferometer, mathematical model of Fabry-Perot reflection spectrum, gas concentration

Authors

S.M.R.H. Hussein, A.Zh. Sakhabutdinov, O.G. Morozov, V.I. Anfinogentov, J.A. Tunakova, A.R. Shagidullin, A.A. Kuznetsov, K.A. Lipatnikov, and A.R. Nasybullin

RESEARCH PAPER

Applicability Limits of the End Face Fiber-optic Gas Concentration Sensor, Based on Fabry-Perot Interferometer

S.M.R.H. Hussein [a], A.Zh. Sakhabutdinov [b,*], O.G. Morozov [b], V.I. Anfinogentov [b], J.A. Tunakova [b], A.R. Shagidullin [c], A.A. Kuznetsov [b], K.A. Lipatnikov [b], A.R. Nasybullin [b]

[a] University of Karbala, Karbala, 56001, Iraq
[b] Kazan National Research Technical University Named After A.N. Tupolev-KAI, 10, K. Marx Str., 420011, Kazan, Russian Federation
[c] Research Institute for Problems of Ecology and Mineral Wealth Use of Tatarstan Academy of Sciences, 28, Daurskaya Str., 420087, Kazan, Russian Federation

Abstract

The mathematical model of the fiber-optic sensor for gas concentration analysis is under study. The sensor is implemented as Fabry-Perot interferometer at the end face of the optical fiber by applying a thin polymer film, which permittivity depends on the tested gas concentration. It is shown, that a change in the properties of the optical fiber or the atmosphere permittivity leads mainly to the spectrum contrast changing and does not change the period and the wavelength shift of its comb. The influence of the polymer film thickness, the environment temperature and humidity on the Fabry-Perot spectrum is analyzed. The necessity of using the temperature and humidity compensation sensors is shown. The method, which determines the permittivity in narrow and wide ranges basing on the comb period and the wavelength shift of Fabry-Perot reflection spectrum, is developed. The relative error of measuring the polymer film permittivity depending on the film thickness for three wavelength ranges (810−890, 1270−1350, and 1510−1590 nm) is estimated. The real achievable relative error in determining the polymer film permittivity is in 0.3−1% FSI, depending on the conditions of the experiment. The mathematical methods and practical recommendations are proposed.

Keywords: Fabry-Perot interferometer, Mathematical model of Fabry-Perot reflection spectrum, Gas concentration

1. Introduction

The implementation of the automatic measuring instruments of gas concentration is one of the strategic priorities, especially important for the ecological safety. For example, in the ecological security projects it is necessary to accurately monitor the leakage of dangerous gases at a storage area to evaluate the potential risks and hazards to human health [1,2], and the environmental safety [3]. The sensors, based on a long period grating, covered with phenol [4] or polystyrene [5] layer, are suggested to achieve these objectives. The silicon photonic sensor, based on a micro-ring resonator coated by a guanidine polymer, is proposed in [6]. Non-dispersive infrared spectroscopic sensor, which is recommended in [7,8], requires a bulky optical absorption cell for achieving high-resolution measurements. The laser absorption spectroscopic methods in the middle infrared range [9] are mainly used for the CO_2 optical fiber sensors. However, the fiber optic components for the middle infrared range, such as light source, photodetector, and even optical fiber itself, are costly [10].

Fiber optic Fabry-Perot interferometer with an open resonator is a classic sensitive element of the gas concentration sensor. It is manufactured by splicing capillary tubes or photonic crystal fibers with a single-mode fiber [11,12]. However, variation

Received 24 March 2022; revised 22 May 2022; accepted 26 May 2022.
Available online 1 August 2022

* Corresponding author.
E-mail address: azhsakhabutdinov@kai.ru (A.Zh. Sakhabutdinov).

https://doi.org/10.33640/2405-609X.3243

of the gas concentration is too small to noticeably change the environment permittivity in the zone of the open interferometer, and is not enough to measure it. The search (or synths) of the transparent material, which refractive index (permittivity) is noticeably sensitive to the concentration of the controlled gas, is the key element of the design of Fabry-Perot interferometer. Fabry-Perot interferometer can be represented as a layered structure consisting of three different homogeneous layers through which a light propagates. A thin film made of a transparent organic polymer material, which permittivity and, hence, refractive index depend on the specific gas concentration, can be used as a sensitive layer. The sensitive layer is in contact with the environment, which allows the polymer material to interact with gas molecules. The interaction of gas and polymer molecules changes the polymer internal structure, thereby changing its permittivity and, as a consequence, its refractive index. According to the Hard Soft Acid Base rule [13,14], the dense polymer film can interact with carbon dioxide molecules at a room temperature and a normal atmospheric pressure by the amino groups which exist in the backbone of the polymer. This interaction is an acid–base equilibrium, it is reversible and leads to the formation of amino formic acid ester and alkyl carbonate [10].

The Fabry-Perot interferometer model [15–17] can be represented as a layered structure consisting of three (or more) different homogeneous layers. A plane monochromatic optical light wave propagates through the layers. The scheme of the Fabry-Perot interferometer with a sensitive element as the thin polymer film at the end face of the optical fiber is shown in Fig. 1.

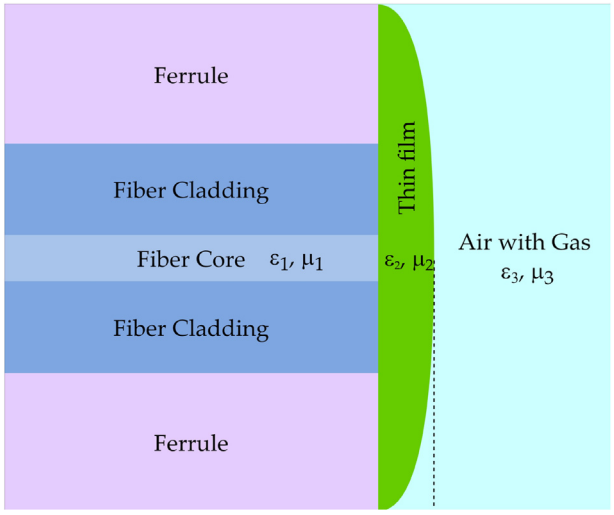

Fig. 1. The sensitive element of gas concentration sensor.

The thin polymer film is a transparent organic polymer material with a thickness of h. The film (is shown by green) is applied to the end face of the optical fiber. The permittivity, hence the refractive index, of the polymer film depend on the tested gas concentration [10,18,19].

The mirrors of Fabry-Perot interferometer are formed due to the difference in refractive indices at two interfaces: between the polymer film and the optical fiber, and between the polymer film and the atmosphere. The polymer film material is selected basing on the requirement that its permittivity must depend on the tested gas concentration. Despite Fabry-Perot interferometers are well described and studied [15,20–22], the completely satisfying results of the applicability limits of Fabry-Perot interferometers as a gas concentration sensor have not been found.

Broadband optical light directed into the optical fiber, reflects from two mirrors, formed by the interfaces, changes its spectral structure and forms the reflection spectrum with periodic increases and decreases of magnitude (like a comb), as shown in Fig. 2.

The contrast of the Fabry-Perot reflection comb, its period, and position along the wavelength axis depend on the parameters of the measuring system, such as the permittivity and the permeability of three substances (fiber, film, and air), and the polymer film thickness. The light transmittance and the light reflectance are found by solving the linear equation system:

$$\begin{bmatrix} 1 & -1 & -1 & 0 \\ -w_2 & -w_1 & w_1 & 0 \\ 0 & e^{-j\kappa_2 h} & e^{j\kappa_2 h} & -e^{-j\kappa_3 h} \\ 0 & w_3 e^{-j\kappa_2 h} & -w_3 e^{j\kappa_2 h} & -w_2 e^{-j\kappa_3 h} \end{bmatrix} \times \begin{bmatrix} r_1 \\ t_2 \\ r_2 \\ t_3 \end{bmatrix} = \begin{bmatrix} -1 \\ -w_2 \\ 0 \\ 0 \end{bmatrix}$$

where κ_i is the wavenumber and w_i is the wave impedance of each layer:

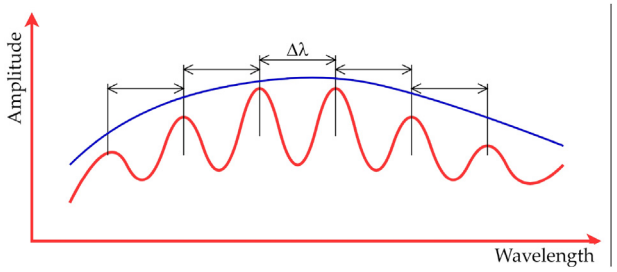

Fig. 2. The Fabry-Perot reflection spectrum (comb).

$$\kappa_i(\lambda, \varepsilon_i, \mu_i) = 2\pi \frac{\sqrt{\varepsilon_i \mu_i}}{\lambda} \ ,$$

$$w_i(\mu_i, \varepsilon_i) = \sqrt{\frac{\mu_i}{\varepsilon_i}} \ ,$$

where ε_1, μ_1, ε_2, μ_2, ε_3, μ_3 are the permittivity and the permeability of the optical fiber core, polymer film, and environment; h is the polymer film thickness; r_1 is the reflection coefficient of the interface between the optical fiber and the polymer film; t_2 and r_2 are the transmittance and reflection between the polymer film and the atmosphere interface; t_3 is the transmittance of the environment; λ is the light wavelength.

The solution of the equation system gives the required transmittance and reflection coefficients as function of the task parameters:

$$\begin{cases} r_1 = \dfrac{\cos\left(\kappa_2 h + \dfrac{j}{2}\ln\left(\dfrac{w_2(-w_1 - w_2 + w_3) + w_1 w_3}{w_2(-w_1 + w_2 + w_3) - w_1 w_3}\right)\right)}{\cos\left(\kappa_2 h + \dfrac{j}{2}\ln\left(\dfrac{w_2(w_1 - w_2 + w_3) - w_1 w_3}{w_2(w_1 + w_2 + w_3) + w_1 w_3}\right)\right)} \\ t_2 = \dfrac{(w_1 + w_2)}{2w_1} - \dfrac{(w_2 - w_1)}{2w_1} r_1 \\ r_2 = \dfrac{(w_3 - w_2)}{(w_3 + w_2)} e^{-2j\kappa_2 h} t_2 \\ t_3 = \dfrac{w_3}{w_2} e^{-j(\kappa_2 - \kappa_3)h} t_2 - \dfrac{w_3}{w_2} e^{j(\kappa_2 + \kappa_3)h} r_2 \end{cases},$$

where all parameters depend on λ, h, ε_i, μ_i.

The main task parameter is the reflection function r_1 (λ, h, ε_i, μ_i) of the interface between the optical fiber and the polymer film. The product of the reflection coefficient r_1 on the original broadband light simulates the Fabry-Perot reflection spectrum. The original light spectrum, which is directed into the Fabry-Perot interferometer, can be described by a Gaussian function:

$$L(\lambda) = A_{\mathrm{L}} \cdot e^{-\frac{(\lambda - \lambda_{\mathrm{L}})^2}{2\sigma^2}} + N \cdot Noise(\lambda),$$

where A_{L} is an amplitude, σ is a width, and λ_{L} is a central wavelength, N is a noise amplitude, and $Noise(\lambda)$ is a noise distribution function.

The Fabry-Perot reflection spectrum is described by the equation:

$$R(\lambda, h, \varepsilon_i, \mu_i) = L(\lambda) \cdot |r_1(\lambda, h, \varepsilon_i, \mu_i)|^2.$$

The dependence of the Fabry-Perot reflection spectrum on the task parameters is a complex transcendental function:

$$R(\lambda, h, \varepsilon_i, \mu_i) = \left(A \cdot e^{-\frac{(\lambda - \lambda_{\mathrm{L}})^2}{2\sigma^2}} + N \cdot Noise(\lambda)\right) \times \times \left|\frac{\cos\left(2\pi\sqrt{\varepsilon_2 \mu_2}\ \dfrac{h}{\lambda} + \alpha\right)}{\cos\left(2\pi\sqrt{\varepsilon_2 \mu_2}\ \dfrac{h}{\lambda} + \beta\right)}\right|^2, \quad (1)$$

where

$$\alpha = \frac{j}{2}\ln\left(\frac{\sqrt{\frac{\mu_2}{\varepsilon_2}}\left(-\sqrt{\frac{\mu_1}{\varepsilon_1}} - \sqrt{\frac{\mu_2}{\varepsilon_2}} + \sqrt{\frac{\mu_3}{\varepsilon_3}}\right) + \sqrt{\frac{\mu_1}{\varepsilon_1}}\sqrt{\frac{\mu_3}{\varepsilon_3}}}{\sqrt{\frac{\mu_2}{\varepsilon_2}}\left(-\sqrt{\frac{\mu_1}{\varepsilon_1}} + \sqrt{\frac{\mu_2}{\varepsilon_2}} + \sqrt{\frac{\mu_3}{\varepsilon_3}}\right) - \sqrt{\frac{\mu_1}{\varepsilon_1}}\sqrt{\frac{\mu_3}{\varepsilon_3}}}\right) \ ,$$

and

$$\beta = \frac{j}{2}\ln\left(\frac{\sqrt{\frac{\mu_2}{\varepsilon_2}}\left(\sqrt{\frac{\mu_1}{\varepsilon_1}} - \sqrt{\frac{\mu_2}{\varepsilon_2}} + \sqrt{\frac{\mu_3}{\varepsilon_3}}\right) - \sqrt{\frac{\mu_1}{\varepsilon_1}}\sqrt{\frac{\mu_3}{\varepsilon_3}}}{\sqrt{\frac{\mu_2}{\varepsilon_2}}\left(\sqrt{\frac{\mu_1}{\varepsilon_1}} + \sqrt{\frac{\mu_2}{\varepsilon_2}} + \sqrt{\frac{\mu_3}{\varepsilon_3}}\right) + \sqrt{\frac{\mu_1}{\varepsilon_1}}\sqrt{\frac{\mu_3}{\varepsilon_3}}}\right) \ .$$

Unfortunately, it is impossible to extract the comb period and the peak position explicitly from Equation (1). A monotonic change in one parameter (the permittivity of one of the layers or the interferometer length) does not lead to a monotonic

Table 1. Task parameters.

	from	to	Denotation
	Permittivity		
Fiber core	$1.9184 \cdot (1 - j \cdot 1.0 \cdot 10^{-10})$	$2.3447 \cdot (1 - j \cdot 1.0 \cdot 10^{-10})$	ε_{F}
Polymer thin film	$3.8000 \cdot (1 - j \cdot 7.0 \cdot 10^{-4})$	$38.000 \cdot (1 - j \cdot 7.0 \cdot 10^{-4})$	ε_{P}
Air	$1.00057 \cdot (1 - j \cdot 1.0 \cdot 10^{-5})$		ε_{A}
	Permeability		
Fiber core	0.9999		μ_{F}
Polymer thin film	0.8660		μ_{P}
Air	1.0001		μ_{A}
	Thickness (μm)		
Polymer thin film	50	150	h

change in the comb period of the Fabry-Perot reflection spectrum or its wavelength; moreover, the shift of the spectrum along the wavelength axis can be on an arbitrary number of periods, including multiple ones.

The polymer film thickness and the permittivity of layers depend on the sensor manufacturing technology and the used materials. The sensitivity of the polymer film to gas concentration, temperature, and humidity of the environment is defined by the polymer film chemical substance. In this regard, the comprehensive investigation of the proposed sensor design is relevant for determining the conditions and limitations of its applicability. These investigations are carried out basing on the proposed mathematical model. The measuring system parameters, which are supposed to be used during the operation, are taken.

Three wavelength ranges (810–890 nm, 1270–1350 nm, 1510–1590 nm), used in optical data transmission networks, corresponding to three optical fiber transparency windows, are chosen. The permittivity and permeability of the substances, the polymer film thickness, and their value ranges are shown in Table 1.

The change of the magnetic permeability of all materials, used in Fabry-Perot interferometer design, can be neglected, since all layers are dielectric, and their ability to polarize in an external magnetic field is absent. The external influence, such as, temperature or humidity, does not affect permeability either. The fiber core permittivity is influenced by the external conditions, such as temperature. Therefore, it is necessary to estimate dependence of the resulting Fabry-Perot spectrum on the fiber core permittivity. The key element of the measuring system is the polymer film. The film thickness is determined during manufacturing, and depends on its temperature (by the coefficient of thermal expansion) and humidity (swelling from moisture). It is assumed, that the film thickness is in the range from 50 to 150 microns. The key parameter of the Fabry-Perot sensor is the polymer film permittivity and its sensitivity to the tested gas concentration. The polymer film permittivity can vary either in a small range or increase by an order of magnitude when the polymer is saturated with the interacted gas. It is assumed, that the real part of the permittivity is varied in the range from 3.8 to 38, while the dielectric loss tangent is assumed constant. All measurements are carried out by analyzing the Fabry-Perot reflection spectrum, obtained as a discrete set, containing a wavelength and an amplitude $\{\lambda_i, A_i\}$ $i = 1, N$, with a sampling step $\Delta\lambda$ and a maximum amplitude A_L. It is assumed that the spectrum analyzer gives 512 spectrum values.

2. Influence of the fiber core permittivity

The temperature coefficient of permittivity is determined by Clausius–Mossotti equation [23,24]. It is about 10^{-6} K^{-1} for gaseous substances, and about 10^{-3} K^{-1} for liquid and solid dielectrics. The temperature change in the range of ±100 K leads to the change in the optical fiber permittivity (ε_F) in the range of ±10% of its regular value under normal conditions. The minimum ε_F value, given in Table 1, corresponds to 90%, and the maximum corresponds to 110% of its regular value equal to $2.3447 \cdot (1 - j \cdot 10^{-10})$, taken as 100%. Fig. 3 shows Fabry-Perot reflection spectra calculated for the wavelength range 1510–1590 nm, for the polymer film thickness $h = 50$ μm, and for three values of the permittivity equal to 90, 100, and 110% of the regular value of ε_F. The incident broadband light spectrum is indicated by the blue line in Fig. 3.

The series of numerical calculations has been simulated for other wavelength ranges and different thicknesses of the polymer film. The change of the fiber core permittivity value in the range of ±10% of its regular value does not lead to a noticeable change in the period or the wavelength of the Fabry-Perot comb. The change of the permittivity of the optical fiber core in the mentioned range leads only to the change of the spectrum contrast. The significant change of ε_F, for example, for 100%, extremely reduces the Fabry-Perot comb contrast. The further increase of ε_F for 200% leads to the spectrum shift on a half of its period, and the maxima and minima of the Fabry-Perot reflection spectrum are swapped. The change in the permittivity of the outer layer ε_A shows the similar transformation of the Fabry-Perot reflection spectrum. The small change (±10%) of the outer layer permittivity does not lead to a noticeable change of the period or the wavelength of the Fabry-Perot comb. The significant change in ε_A (both increase or decrease) leads to the spectrum shift on a half of the comb period. The simultaneous change of the permittivity of the optical fiber and the environment in the range of ±10% has the similar character.

In industrial exploitation, the optical fiber core permittivity cannot change for more than 10%. Only temperature can affect the optical fiber permittivity. In most cases, the change of the atmosphere permittivity can be neglected, assuming that its maximum deviation is less than ±1% of its regular value under any external influences.

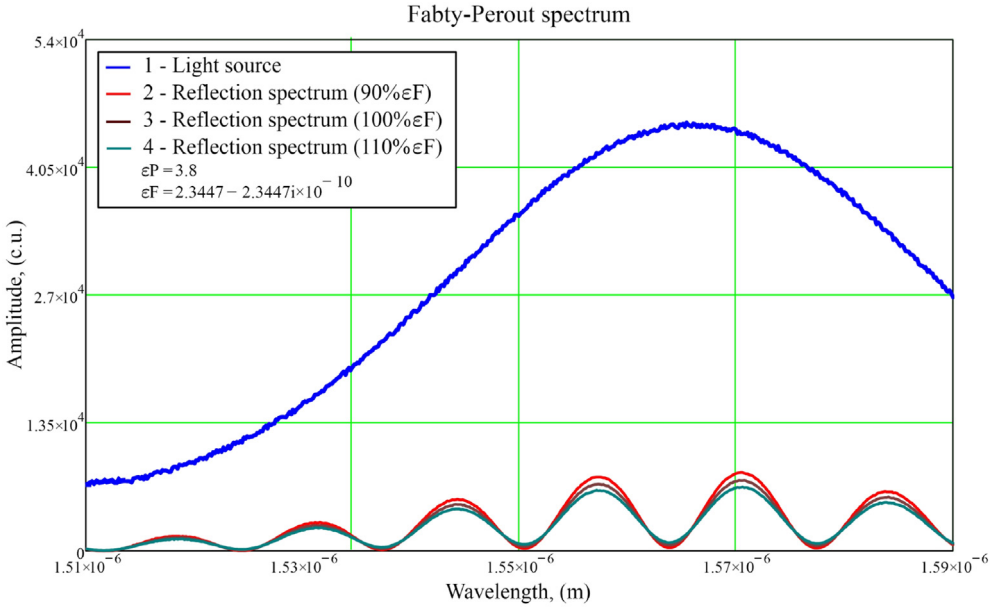

Fig. 3. The results of spectrum calculations: 1 — source light; the Fabry-Perot comb for the wavelength range 1510–1590 nm, for the polymer film thickness h = 50 μm, and for three permittivity values of the optical fiber: 2 — at 90% of ϵ_F; 3 — at $\epsilon_F = 2.3447 \cdot (1 - j \cdot 10^{-10})$; 4 — at 110% of ϵ_F.

The possible changes in contrast of the Fabry-Perot comb resulting from temperature fluctuations impose minor restrictions; therefore, it is necessary to use amplitude measurement methods with caution and to use extra compensation sensors. Small variations (±10%) of the permittivity of the optical fiber or atmosphere affect only the change in contrast of the Fabry-Perot comb and very insignificantly affect its period or wavelength. This makes it possible to exclude the temperature control of the optical fiber and the environment from consideration and focus only on the analysis of the temperature and parameters of the polymer film. The main efforts in developing a method for estimating changes in the polymer film permittivity should be concentrated on the analysis of the Fabry-Perot comb period and its wavelength.

3. Influence of the wavelength range

The fiber optic spectrum analyzer, designed for the wavelength range 810–890 nm, is a lot cheaper than the comparable equipment designed for the wavelength range 1270–1350 nm or 1510–1590 nm. Increasing the resolution of the spectrum analyzer also leads to a significant increase in costs, since it requires more complicated and expensive hardware components, especially for the wavelength range 1510–1590 nm. In other words, the cost of the fiber-optic spectrum analyzers increases both with increasing of the resolution and the operating wavelength. The proposed mathematical model allows investigating the applicability of the suggested gas concentration sensor not only for various wavelength ranges, but also for an arbitrary wavelength, which allows selecting the equipment, based on technical and economic requirements. The period of the Fabry-Perot comb has a quadratic dependence on the wavelength, according to the theoretical models for determining Free Spectral Range (FSR) of the interferometer [18]:

$$\Delta\lambda = \frac{\lambda^2}{2\sqrt{\varepsilon_P \mu_P} h},$$

where Δλ is FSR, and it is defined as the period of the Fabry-Perot spectrum comb.

The series of numerical calculations for three wavelength ranges (810–890, 1270–1350, and 1510–1590 nm), with the polymer film thickness h = 50 μm and three values of the optical fiber permittivity (90, 100, and 110% of ε_F) has been simulated. The resulting spectra are shown in Fig. 4; parts of the spectra that are not included in the indicated wavelength ranges are excluded from the figure for clarity. The results of the investigation, obtained by switching the wavelength range, clearly demonstrate the increase of the Fabry-Perot comb period with the wavelength increasing.

4. Influence of the polymer film thickness

The sensing element ability of the suggested gas concentration sensor directly depends on the

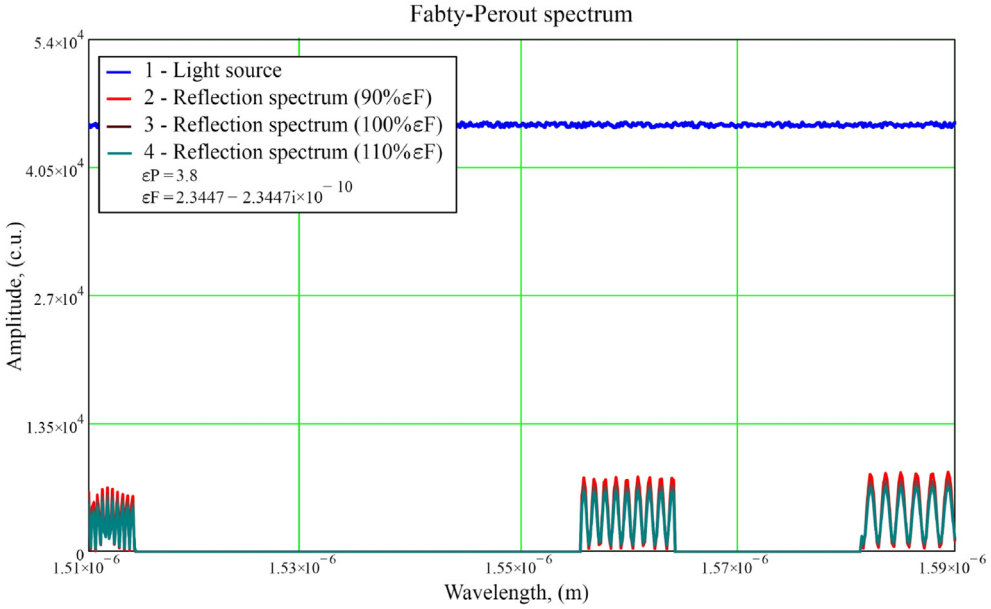

Fig. 4. The results of spectrum calculations: 1 — source light; the Fabry-Perot comb for the wavelength range 810–1590 nm, for the polymer film thickness $h = 50$ μm, and for three permittivity values of the optical fiber: 2 — at 90% of ϵ_F; 3 — at $\epsilon_F = 2.3447 \cdot (1 - j \cdot 10^{-10})$; 4 — at 110% of ϵ_F.

selected substance and thickness of the polymer film. Hence, it is necessary to study the influence of the polymer film thickness, and the affection of the linear thermal expansion coefficient of the polymer on the resulting Fabry-Perot comb. It allows assessing the need to use extra temperature compensation sensors.

The polymer film thickness varies in the range from 50 to 150 μm while the values of other system parameters are fixed. The calculated Fabry-Perot reflection spectra are shown in Fig. 5.

The results of calculations show that an increase in the thickness of the polymer film leads to a decrease in the period of the Fabry-Perot comb. This dependence is the same for all wavelength ranges.

On one hand, the large polymer film thickness increases the range of the film permittivity, which depends on gas concentration. The greater film

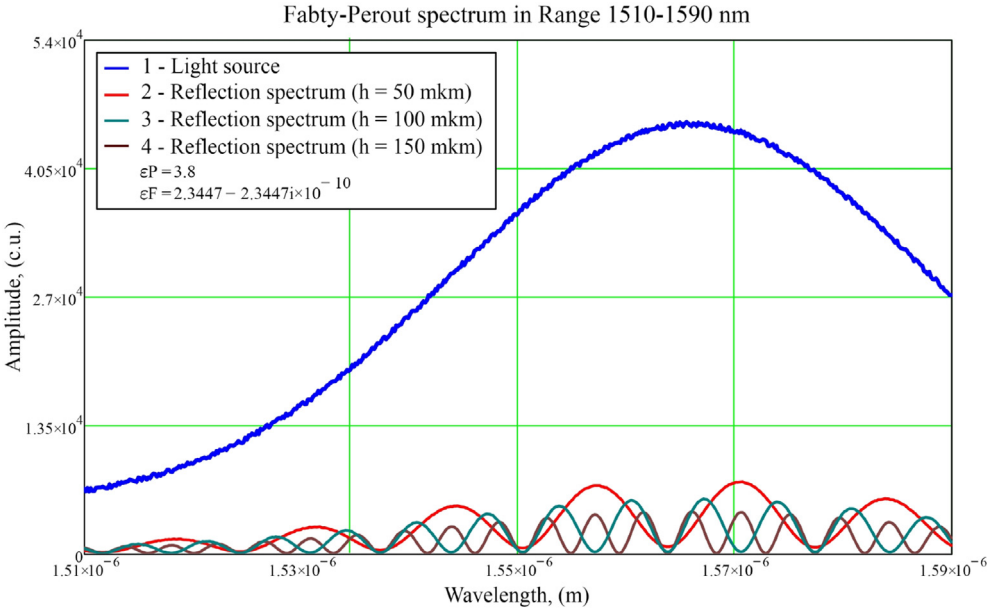

Fig. 5. The results of spectrum calculations: 1 — source light; the Fabry-Perot comb for the wavelength range 1510–1590 nm, and for three thickness values of the polymer film: 2 — $h = 50$ μm; 3 — $h = 100$ μm; 4 — $h = 150$ μm.

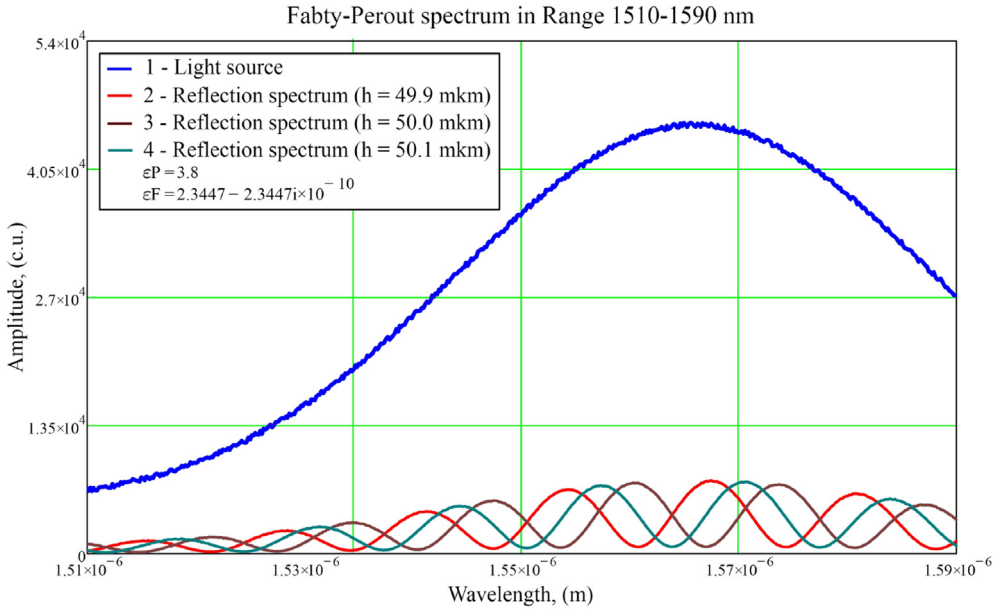

Fig. 6. The results of spectrum calculations:1 — source light; the Fabry-Perot comb for the wavelength range 1510–1590 nm, and for three thickness values of the polymer film: 2 — $h = 49.9$ μm; 3 — $h = 50$ μm; 4 — $h = 50.1$ μm.

volume contains more active points to attach the gas molecules to the polymer. On the other hand, the gradient of gas molecules concentration appears across the film thickness, with the maximum value near the polymer–environment interface and the minimum value near the polymer–fiber interface. The gradient of gas molecules concentration in the film leads to the appearance of the permittivity gradient across the film thickness. The affection of the permittivity gradient across the film thickness is not considered here, but it is planned for the next researches.

The linear thermal expansion coefficient of the polymers used as the gas-absorbing films is in the range from $0.5 \cdot 10^{-5}$ to $2 \cdot 10^{-5}$ K^{-1}. The maximum value of the linear thermal expansion coefficient means that the thickness of the polymer film changes according to the relation $h \cdot (1 + 2 \cdot 10^{-5} \cdot \Delta T)$, where ΔT is the maximum value of the temperature shift. Assuming that the temperature of the gas

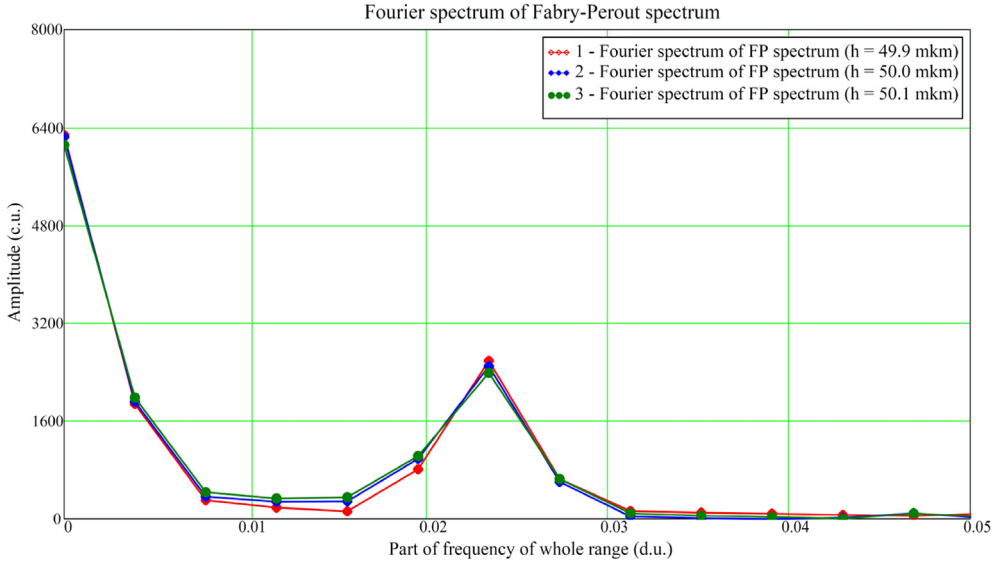

Fig. 7. The Fourier spectra of the Fabry-Perot reflection spectra calculated for the wavelength range 1510–1590 nm, for three thickness values of the polymer film: 1 — $h = 49.9$ μm; 2 — $h = 50$ μm; 3 — $h = 50.1$ μm.

concentration sensor varies in the range of ±100 K, then the polymer film thickness varies in the range of $h \pm h \cdot 0.002$.

Calculations show that the change of the polymer film thickness even in such small range leads to the noticeable shift of the Fabry-Perot reflection spectrum, Fig. 6.

Even though the change of the film thickness is only 0.2%, the shift of Fabry-Perot comb is quite noticeable. The change of the Fabry-Perot comb period can be estimated by the Fourier transform applied to the Fabry-Perot spectrum. The Fourier spectrum is performed using the fast Fourier transform algorithm, under the assumption that the fiber-optic spectrum analyzer gives 2^m numerical values of the spectrum in the matrix form $\{\lambda_i, A_i\}$, $i = 1, 2^m$, containing two vectors — the wavelength and the amplitude, Fig. 7.

The dimensionless value of the Fabry-Perot comb frequency is used as the abscissa axis in Fig. 7. It determines the fraction of the difference frequency of the whole spectrum range. This notation is used to simplify the further explanation.

The frequency which is determined only by the maximum value of the Fourier spectrum means that the error in determining the frequency of the comb is not less than the spectrum sampling frequency, which is determined by the resolution of the optical spectrum analyzer. The frequency of the Fabry-Perot comb is refined by the following algorithm. The maximum value of the amplitude corresponding to the frequency of the Fabry-Perot comb is determined in the Fourier spectrum. Three points $\{f_1, y_1\}$, $\{f_2, y_2\}$, $\{f_3, y_3\}$ of the Fourier spectrum are determined. The point $\{f_2, y_2\}$ is the frequency and amplitude of the Fourier spectrum at the maximum point; $\{f_1, y_1\}$ and $\{f_3, y_3\}$ are the same values at the left and the right points, respectively. A parabola through three points $\{f_i, y_i\}$ is drawn, and the comb frequency is determined as the abscissa of the parabola center according to:

$$a = \frac{y_3(f_2 - f_1) - f_3(y_2 - y_1) - f_2 y_1 + f_1 y_2}{f_3(f_3 - f_1 - f_2) + f_1 f_2},$$
$$b = \frac{y_2 - y_1}{x_2 - x_1} - a(x_1 + x_2), \qquad (2)$$
$$f = -\frac{b}{2a}.$$

where f is the desired frequency, a and b are the coefficients of the second and first orders of the parabola.

The numerical analysis shows, that the deviation of the Fabry-Perot comb frequency when the film thickness changes by 1/500 of its unperturbed length of 50 μm does not exceed 0.5% in the wavelength range 1510–1590 nm, 2% in the range 1270–1350 nm, and 0.24% in the range 810–890 nm. Changing the film thickness to 100 and 150 μm slightly reduces the error in determining the Fabry-Perot comb frequency. It should be noted that increasing the film thickness reduces the error in determining the Fabry-Perot comb frequency. However, this effect is insignificant. According to the performed calculations, it can be concluded that the Fabry-Perot sensor in the wavelength ranges 810–890 and 1510–1590 nm provides a smaller error in determining the comb frequency, than in the wavelength range 1270–1350 nm. The error in determining the Fabry-Perot comb frequency can be reduced by increasing the thickness of the polymer film.

The error in determining the Fabry-Perot comb frequency with a possible drift of the polymer film thickness caused by the change of the external temperature does not exceed 0.5%. The Fabry-Perot comb frequency has non-monotonic dependence on the polymer film permittivity. The error in determining the Fabry-Perot comb frequency affects the error in determining the permittivity. Therefore, it is necessary to use the temperature compensation techniques to improve accuracy. The temperature compensation techniques are not considered in the framework of this study.

5. The determination of the polymer film permittivity in a narrow range

The principal parameter of measurement of this sensor design, which depends on the gas concentration, is the permittivity of the polymer film. The character of the Fabry-Perot comb modification, when the permittivity changes by 5 and 10% of its regular value $|\varepsilon P| = 3.8$, at a film thickness 50 μm, in the wavelength range 1510–1590 nm, is shown in Fig. 8.

The change in the polymer film permittivity leads to the simultaneous change in the Fabry-Perot comb frequency and its position along the wavelength axis. Initially, it seemed reasonable to build the dependence of the polymer film permittivity as a function of two variables — the shift of the spectrum and the Fabry-Perot comb frequency. Moreover, the Fabry-Perot comb frequency was planned to be determined by constructing and analyzing the Fourier spectrum of the Fabry-Perot comb, with the refinement of the comb frequency according to (2). The shift of the Fabry-Perot spectrum was determined as the shift of the mass center of a flat figure

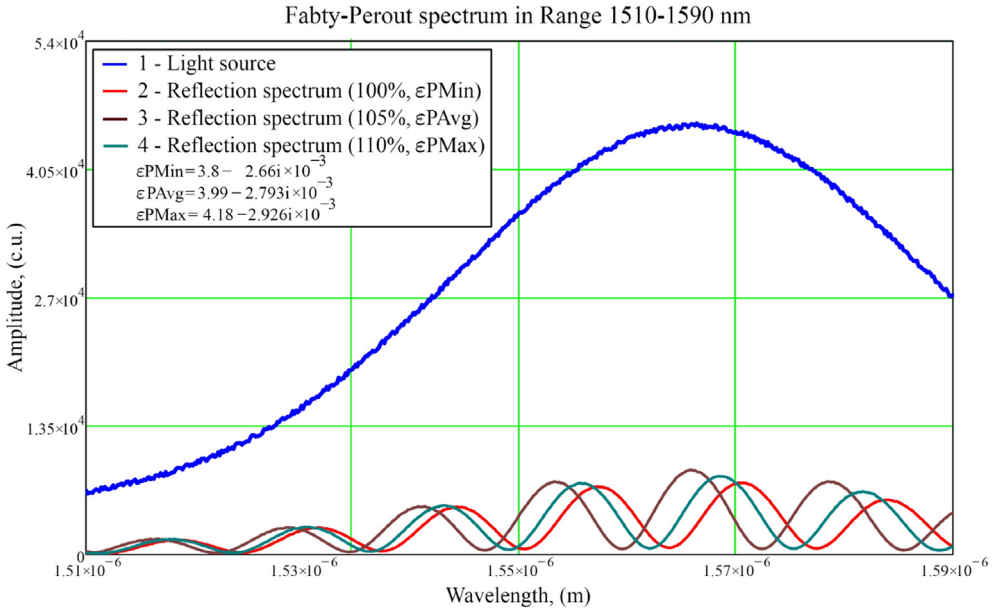

Fig. 8. The calculated spectra: 1 — light source spectrum; the Fabry-Perot comb, calculated for the wavelength range 1510–1590 nm, for three permittivity values of the polymer film: 2 — $\epsilon_{PMin} = 100\%$; 3 — $\epsilon_{PAvg} = 105\%$; 4 — $\epsilon_{PMax} = 110$.

formed by the Fabry-Perot spectrum and the wavelengths boundaries of the range and abscissa axis. The coordinate of the mass center of the Fabry-Perot comb, obtained from the discrete dataset, was determined by the formula:

$$s = \frac{2}{\lambda_{2^m} - \lambda_1} \frac{\sum_{i=1}^{2^m-1} (\lambda_{i+1}^2 - \lambda_i^2)(A_{i+1} + A_i)}{\sum_{i=1}^{2^m-1} (\lambda_{i+1} - \lambda_i)(A_{i+1} + A_i)},$$

where the factor before the ratio normalizes the value of the mass center to a dimensionless unit, in the range from zero to one. The required dependence of the polymer film permittivity was determined by a function:

$$\varepsilon_P = F(f, s). \quad (3)$$

The analytical form of the equation above is determined by the nature of this dependence. To determine the analytical form of function (3) for the film permittivity in range ε_{PMin} to ε_{PMax}, the correlation of the film permittivity with the frequency and the mass center of the Fabry-Perot comb is calculated for all wavelength ranges and the polymer film thicknesses. It is assumed, that the value of the polymer film permittivity varies in the range of ±10%. The calculation results for the film thickness 50 μm, and the film permittivity $|\varepsilon_{PMin}| = 3.80$, $|\varepsilon_{PAvg}| = 3.99$, $|\varepsilon_{PMax}| = 4.18$, which are 100, 105 and 110%, respectively, are shown in Fig. 9. Similar dependencies are calculated for the thicknesses of polymer films equal to 100 and 150 μm, as it is shown in Fig. 10 and Fig. 11. The analysis of the calculation results shows that the correlation of the polymer film permittivity from the comb frequency and the mass center of the Fabry-Perot spectrum resembles a flattened 3D spiral. The change in permittivity by 10% leads not only to the shift of the comb for several periods, but also to the non-monotonic change in the comb period. More detailed information about the nature of the correlation of the permittivity from the frequency and mass center of the Fabry-Perot comb can be obtained from the phase sections "frequency vs permittivity", "mass center vs permittivity" and "frequency vs mass center", as it is shown in Fig. 12. Up to five different values of the permittivity can correspond to one measured value of the Fabry-Perot comb frequency (Fig. 12,*a*), and one measured value of the mass center can correspond to any of the permittivity values located on the dependence (Fig. 12,*b*). The phase section "frequency vs mass center" (Fig. 12,*c*) allows limiting this uncertainty by two different permittivity values, but does not eliminate it. The presence of self-intersections on the phase section "frequency vs center of mass" (Fig. 12,*c*) does not allow to unambiguously determine the value of the permittivity from two measured values of the frequency and mass center, since the same set of values corresponds to two different permittivity values, located on the adjacent

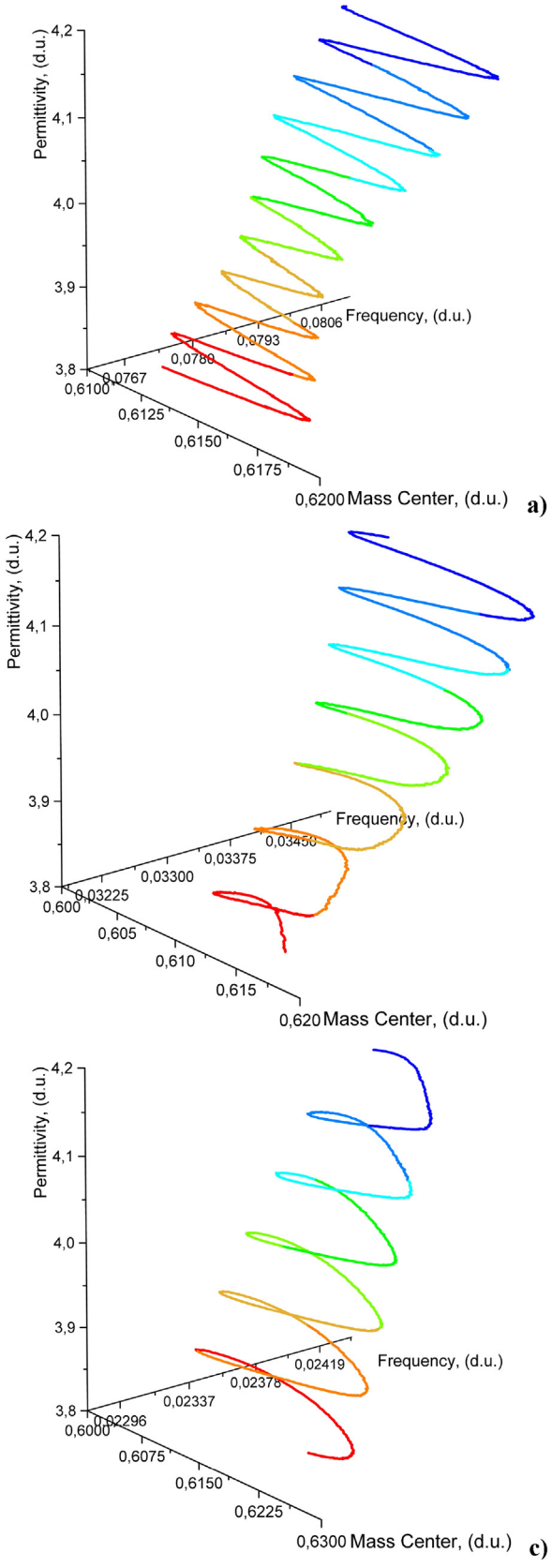

Fig. 9. The calculating results of the dependence of the film permittivity ϵ_P in the range of values of 100–110% at the polymer film thickness h = 50 μm for three wavelength ranges: a) 810–890 nm; b) 1270–1350 nm; c) 1510–1590 nm.

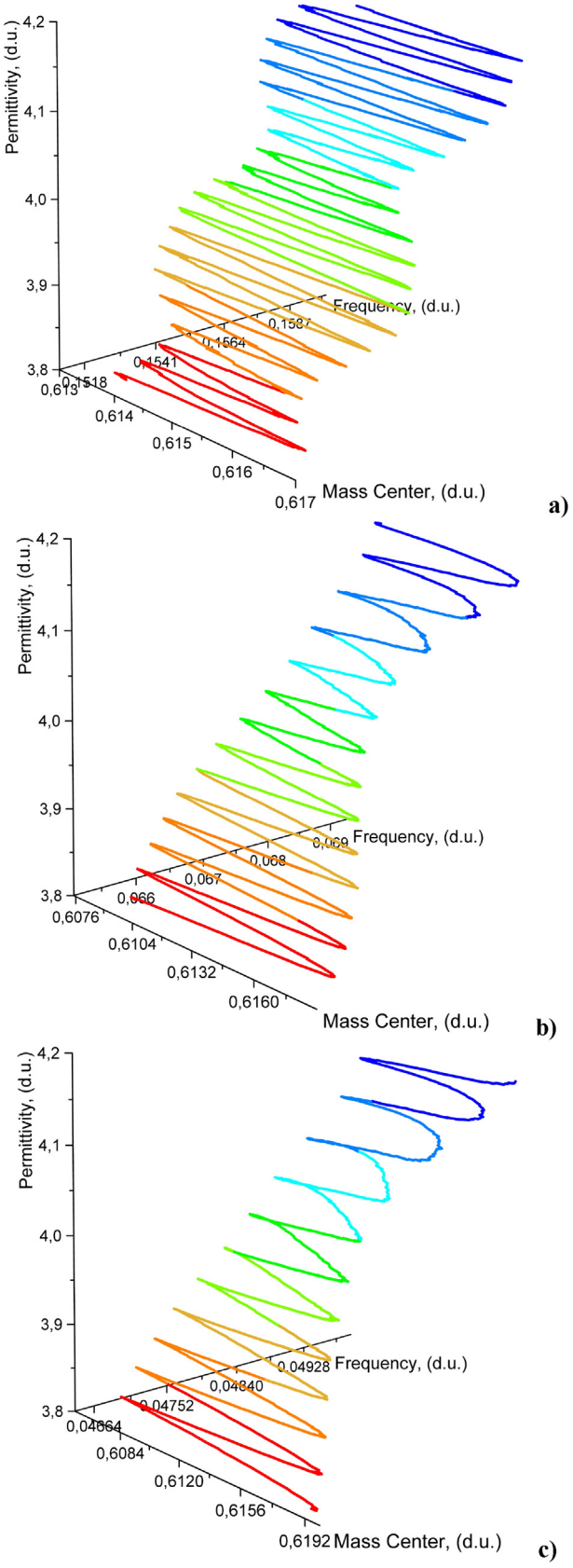

Fig. 10. The calculating results of the dependence of the film permittivity ϵ_P in the range of values of 100–110% at the polymer film thickness h = 100 μm for three wavelength ranges: a) 810–890 nm; b) 1270–1350 nm; c) 1510–1590 nm.

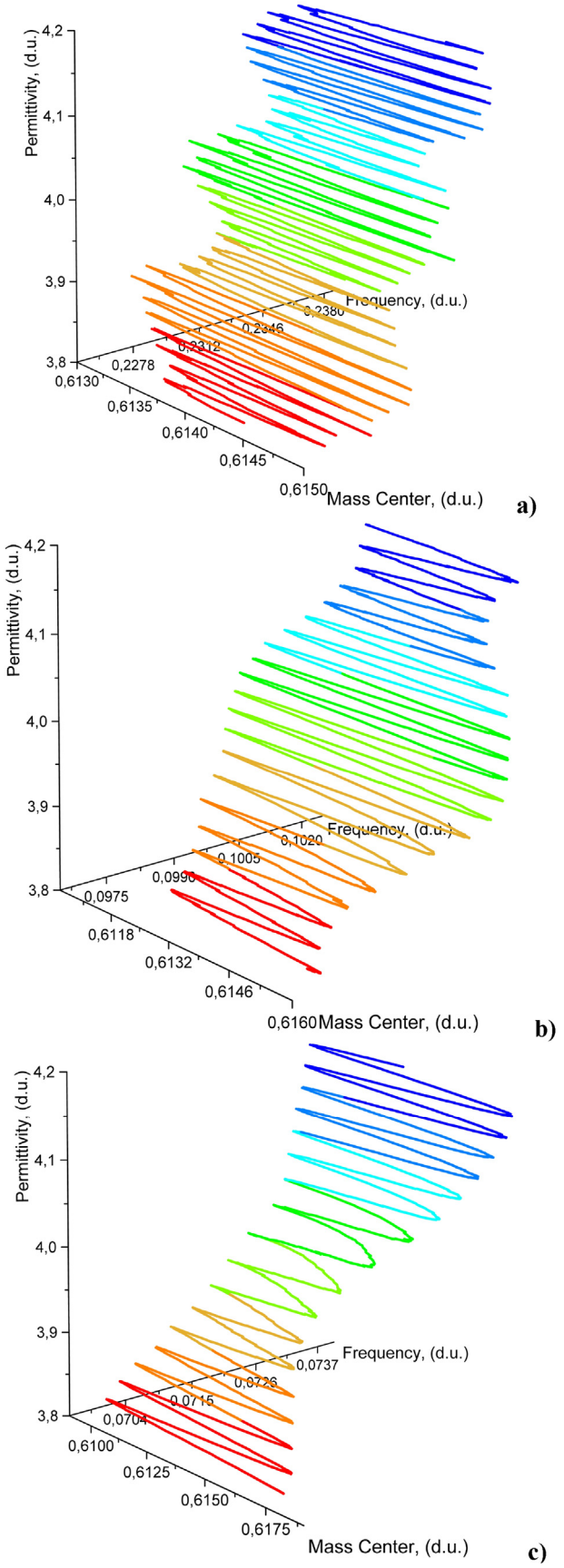

spiral coils. The step of this spiral dependence along the permittivity axis determines the uncertainty value.

Restricting the range of the permittivity variation to ±1% of its initial value allows eliminating this uncertainty, since in this case, the curve in the phase section of the "frequency vs mass center" does not intersect itself. It allows determining the permittivity value unambiguously. The problem can be solved by the selection of the specific polymer film material, which provides its permittivity change in the range of ±1% with the change of the gas concentration in the measurement range. At the same time, it imposes additional restrictions on the accuracy of the permittivity determining.

The phase sections of "frequency vs permittivity", when the permittivity varies in the range of 100–110% (for the range 1510–1590 nm) are shown in Fig. 13, and with the film thickness equal to 100 and 150 μm are shown in Fig. 13,*a* and Fig. 13,*b*, respectively. The phase section for the range 810–890 nm at the film thickness equal to 150 μm is shown in Fig. 13,*c*.

The increase in the polymer film thickness or the transition to the shorter wavelength range reduces the ambiguity of the permittivity correlation with the Fabry-Perot comb period. The consistent comparison of Fig. 12,*a*, Fig. 13,*a*, and Fig. 13,*b* shows that the increase in the polymer film thickness while maintaining all other parameters "straightens" the permittivity correlation with the comb period and reduces the ambiguity. The change in the wavelength range from 1510 to 1590 to 810–890 nm leads to the greater straightening of this correlation, but does not eliminate the fluctuations.

The approximation of the permittivity correlation with the Fabry-Perot comb frequency by the fourth-degree polynomial allows to interpolate with an absolute error not exceeding $2 \cdot 10^{-6}$, Fig. 14,*a*. In this case, the relative error in determining the permittivity based on the calculated value of the Fabry-Perot comb frequency using the approximating curve, does not exceed 0.32% for the entire measurement range.

The switching of the wavelength range between 1270 and 1350 or 810–890 nm does not reduce the absolute error of the permittivity approximation by the frequency, and does not reduce the relative error in determining its value by the approximating

Fig. 11. The calculating results of the dependence of the film permittivity ϵ_P in the range of values of 100–110% at the polymer film thickness h = 150 μm for three wavelength ranges: a) 810–890 nm; b) 1270–1350 nm; c) 1510–1590 nm.

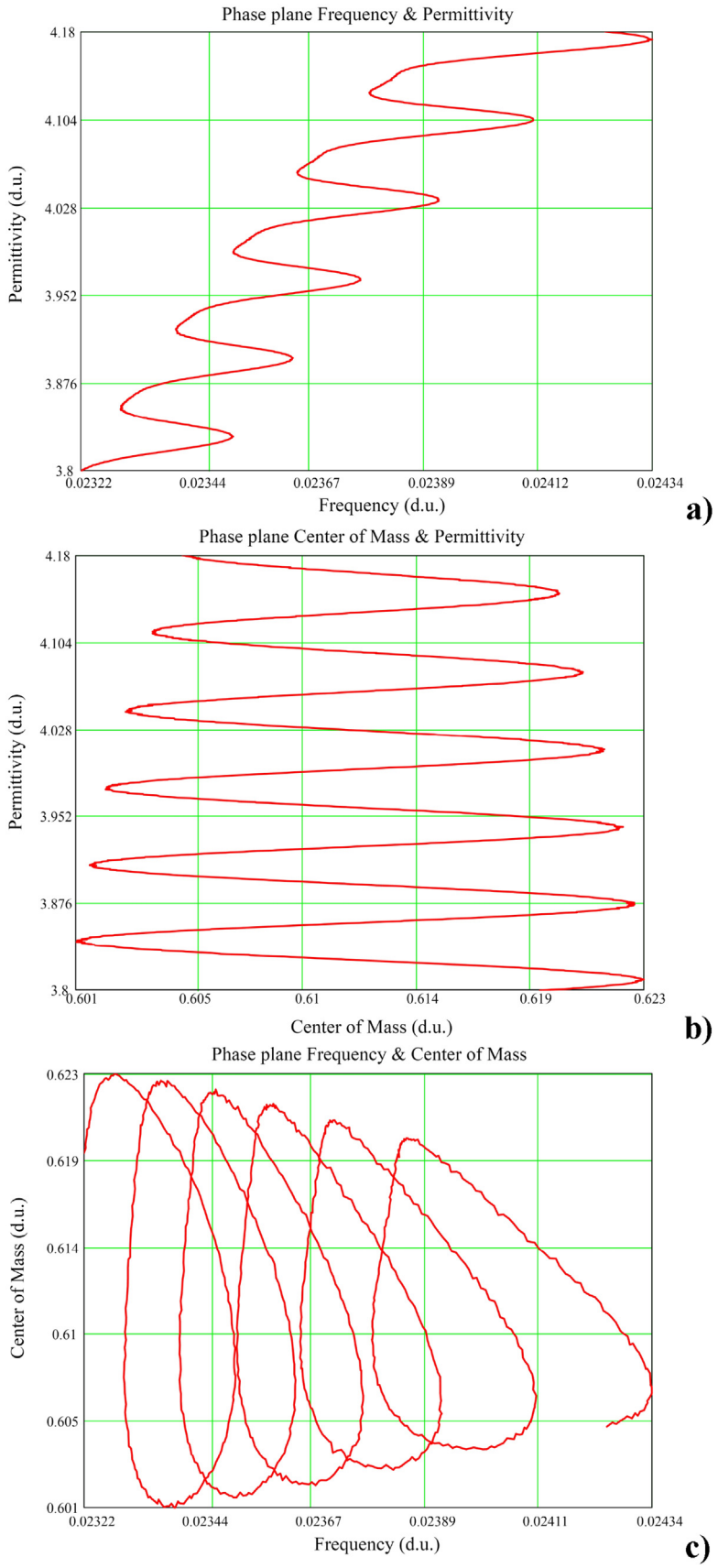

Fig. 12. The phase sections for polymer film permittivity in the range 100–110% at the polymer film thickness h = 50 μm for the wavelength range 1510–1590 nm: a) frequency vs permittivity; b) center of mass vs permittivity; c) frequency vs center of mass.

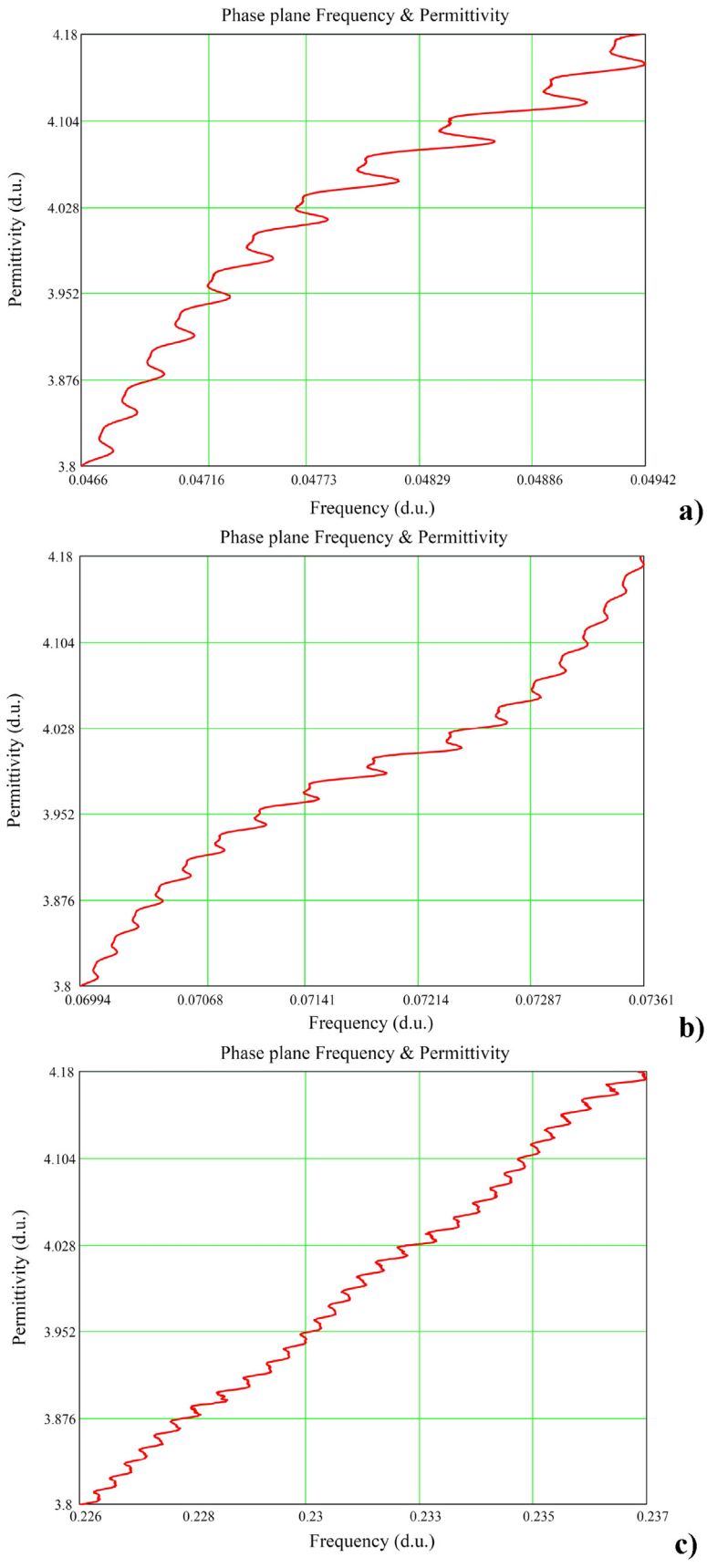

Fig. 13. The phase sections "frequency vs permittivity" for the polymer film permittivity in the range 100–110% for the wave ranges and the film thicknesses: a) 1510–1590 mn, h = 100 μm; b) 1510–1590 nm, h = 150 μm; c) 810–890 nm, h = 150 μm.

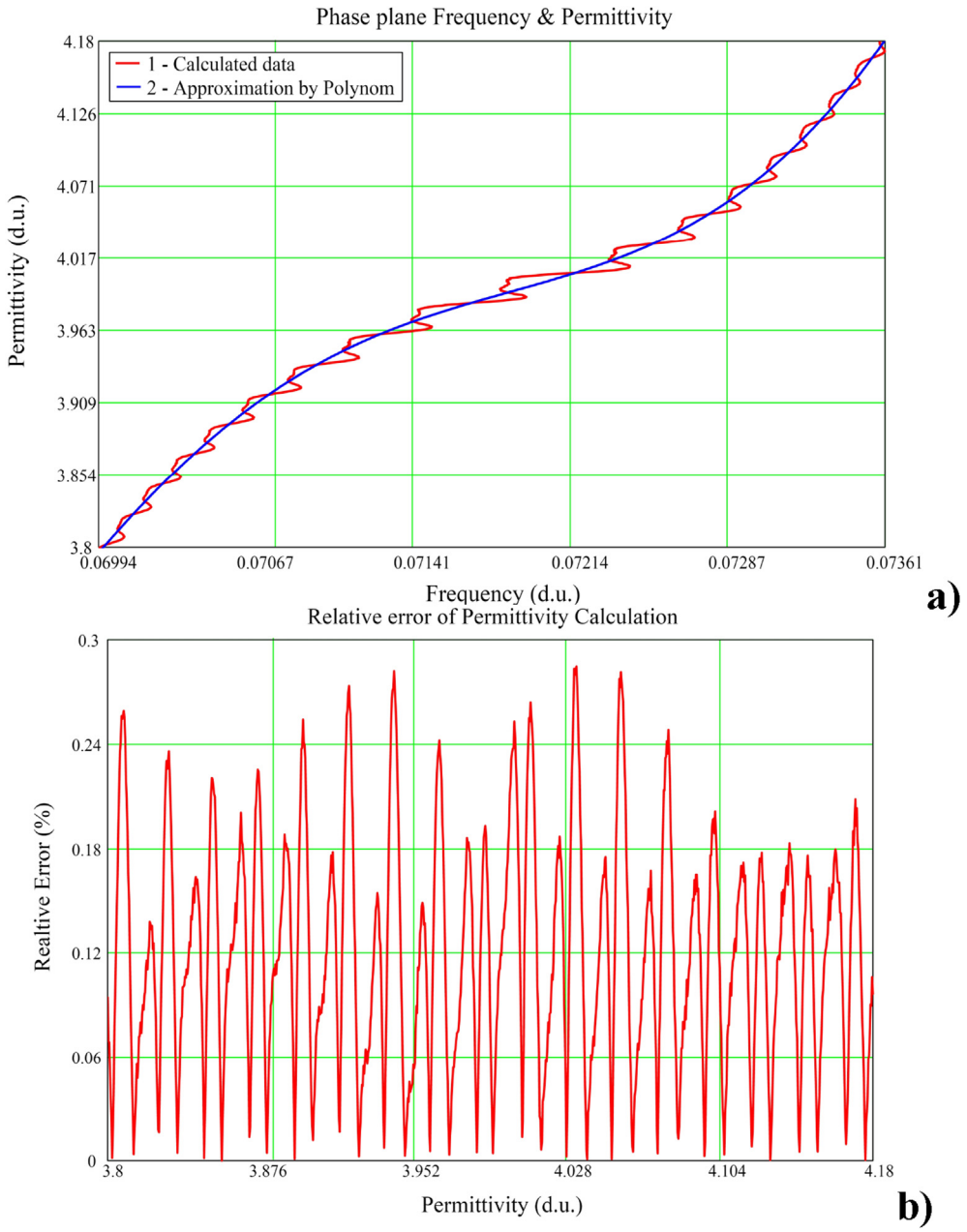

Fig. 14. Approximation for the permittivity in the wavelength range 1510–1590 nm and film thickness h = 150 μm: a) polynomial approximation of the permittivity on the frequency of the Fabry-Perot spectrum comb; b) the relative error in determining the dielectric constant.

curve. The maximum relative error in both cases does not exceed 0.32% FSI.

6. The determination of the polymer film permittivity in the wide range

In parallel with the mathematical model research, our team carried out the laboratory experiments. The experiment results show, that the permittivity can vary beyond the limit of 10%. The experiments with the polymer film made from the polyvinyl alcohol, when it is used as the humidity sensor, show that the polyvinyl alcohol film ability to attach hydroxyl groups can change its permittivity for 7–8 times. The polyvinyl alcohol permittivity in the dry condition does not exceed 3.8, in contrast, the water permittivity is 80. The saturation of the polyvinyl alcohol film with water increases the film permittivity to 20, 30, or more. In this regard, it is advisable to assess the error in determining the permittivity in a wide range (from 100 up to 1000% of its regular value). Let us assume, that the minimum and

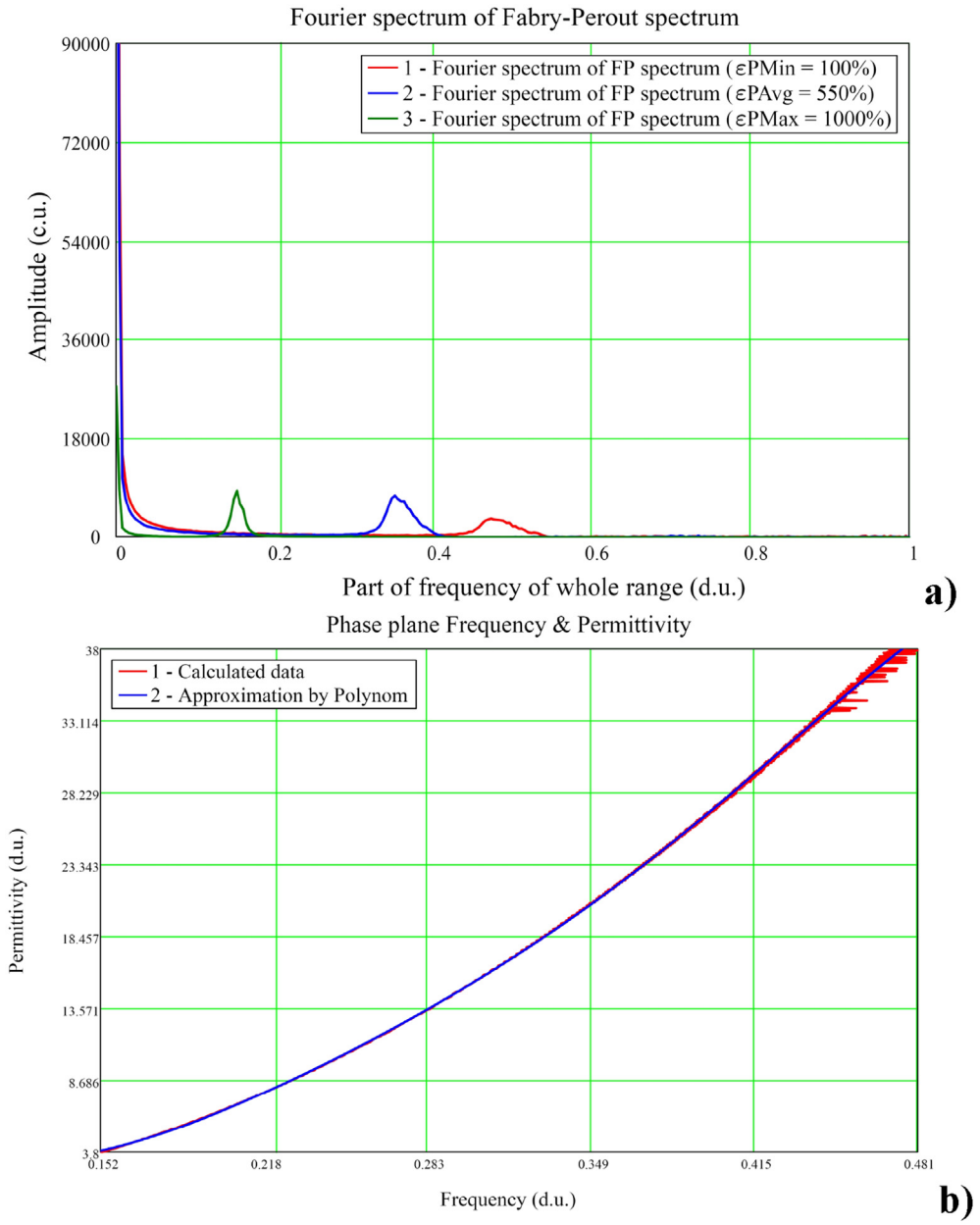

Fig. 15. a) Fourier spectra of the Fabry-Perot combs, calculated for the wavelength range 810–890 nm, and for polymer film thickness h = 100 μm for three permittivity values: 1 — ϵ_P = 100%; 2 — ϵ_P = 550%; 3 — ϵ_P = 1000%; b) approximation of the permittivity for the wavelength range 810–890 nm and the film thickness h = 100 μm.

maximum values of the polymer film permittivity differ by 900%. So, the minimum value is $|\varepsilon_{PMin}| = 3.8$ and the maximum value is $|\varepsilon_{PMax}| = 38.0$, that is 100 and 1000%, respectively. The film thickness varies in the set of 50, 100, and 150 μm for all wavelength ranges. The numerical analysis is performed for three thicknesses of the polymer film, in the wavelength range 1510–1590 nm, with the change in the film permittivity in the range from 100 to 1000%.

The worst error in determining the film permittivity is obtained for the film thickness 50 μm, and it does not exceed 5% FSI. The twofold increase in the polymer film thickness up to 100 μm more than twice reduces the error in determining the film permittivity; the maximum error, in this case, does not exceed 2% FSI. The increase of the film thickness to 150 μm allows halving error to 1.2%.

The transition to the wavelength range 1270–1350 nm reduces the relative error in determining the polymer film permittivity to 3% at the film thickness of 50 μm; more than 1% at the thickness of 100 μm; and less than 0.8% at the thickness of 150 μm.

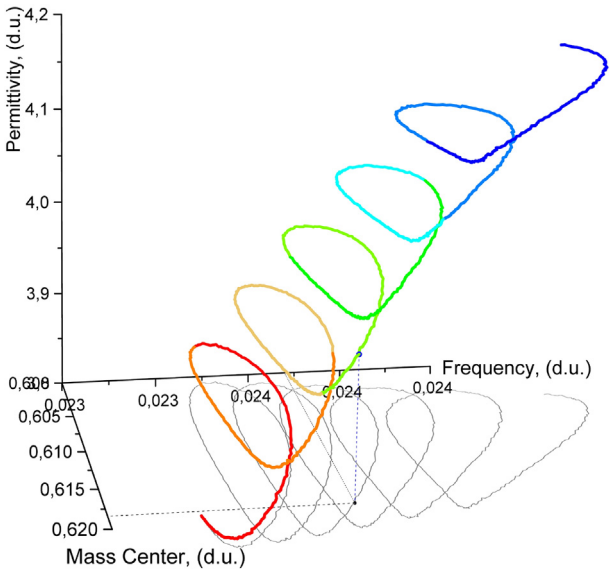

Fig. 16. Determination of the permittivity value from the comb frequency and the center of mass of the Fabry -Perot spectrum.

The transition to the wavelength range 810–890 nm seemed promising since even for the polymer film thickness of 50 μm, the maximum relative error in determining the polymer film permittivity did not exceed 0.8% FSI. However, the polymer film thickness doubling to 100 μm leads to the smearing of the frequency peak in the Fourier spectrum of the Fabry-Perot comb, and to the impossibility of determining its position by three top points, Fig. 15. It increases the maximum relative error of the permittivity determination closer to the upper measurement limit, up to 3.5% FSI. The further increasing of the polymer film thickness in the range 810–890 nm leads to even greater uncertainty in determining the frequency of the Fabry-Perot spectrum comb and increases the measurement errors.

7. Observation in time

Let us return to the analysis of the film permittivity dependence on the comb frequency and the mass center of the Fabry-Perot reflection spectrum, which resembles a flattened 3D spiral. Assume that the frequency of measurements provides the parameter monitoring speed, which guarantees continuities of the permittivity change. That is, two consecutive measurements guarantee that the polymer film permittivity value, calculated by the frequency and the mass center, does not jump from one coil of the spiral to another.

If the proposed assumption is fulfilled, the uncertainty arising when determining the polymer film permittivity in the self-intersection points of the phase section "frequency vs mass center" can be resolved by choosing the value that is closer to the previous measured one.

The task of ambiguity of the polymer film permittivity determining after the first measurement step is solved similarly. If the first measurement gives an ambiguity in determining the measured value, it is corrected by subsequent measurements in dynamics over time.

The complexity of this approach lies in the difficulties of choosing the analytical form of the approximation function $\varepsilon_P = F(f, s)$, which describes a 3D curve in space. It is necessary to form the dependence of the polymer film permittivity on the comb frequency and the mass center of the Fabry-Perot comb with the sufficiently detailed sampling during the calibration of the measurement system. For each measurement, the point with the frequency and mass center (f^*, s^*) is determined, which allows finding the nearest point in the phase section, Fig. 16, and restoring the value of the polymer film permittivity. The ambiguity of the calculated value, in case when the point is located close to the curve self-intersection area of the phase section, is resolved according to the above-proposed algorithm.

The disadvantage of the proposed approach is the need for the detailed sensor calibration and the storage of the sensor calibration curve in the measuring system memory.

8. Conclusion

The mathematical model of the fiber-optic gas concentration sensor, based on the Fabry-Perot interferometer, formed on the end face of the optical fiber by applying the thin polymer film, which permittivity depends on the tested gas concentration, is proposed. The main dependencies and patterns are revealed. The influence of the permittivity drift of the optical fiber and atmosphere on the measurement results is investigated. The influence of the polymer film thickness on the reflection spectrum of the Fabry-Perot interferometer is analyzed. The small changes (no more than 10%) in the permittivity of the optical fiber or atmosphere influence only the contrast of the Fabry-Perot reflection spectrum and do not affect its period or spectrum shift along the wavelength. It allows neglecting the drift of the fiber temperature and the external atmosphere temperature and focusing on controlling the polymer film parameters and characteristics. The effect of the polymer film thermal expansion on the resulting spectrum is investigated. The change of the temperature in the range of ±100 K requires an additional sensor for temperature compensation, since the thermal expansion coefficient of the polymer film significantly impacts on its

thickness, and as a result on the Fabry-Perot comb period. The proposed mathematical apparatus makes it possible to investigate the phenomenon in detail for various film materials and temperature ranges. The problem of ambiguity in determining the polymer film permittivity by the measured values of the comb period and the shift of the Fabry-Perot reflection spectrum is disclosed. The technique for determining the value of the permittivity in narrow and wide ranges, based on the Fabry-Perot reflection comb period and its spectrum shift, is developed. The limitations and methodological errors of the proposed method are determined. The estimation of the relative measurement error in the permittivity for the wavelength ranges 810–890, 1270–1350, and 1510–1590 nm, depending on the polymer film thickness, is made. The real achievable error in determining the polymer film permittivity can be no more than 0.3% FSI in the narrow measuring range, and no more than 1% when the permittivity value changes by an order of magnitude.

Conflict of interest

The authors declare no conflict of interest.

Acknowledgements

The work was supported by the Ministry of Science and Higher Education under the "Priority 2030" program and R&D reg. number AAAA-A20-120122490071-1 (Agreement No. 075-03-2020-051, Topic No. fzsu-2020-0020).

References

[1] E.R. Siirila, A.K. Navarre-Sitchler, R.M. Maxwell, J.E. McCray, A quantitative methodology to assess the risks to human health from CO2 leakage into groundwater, Adv Water Resour. 36 (2012) 146–164, https://doi.org/10.1016/j.advwatres.2010.11.005.
[2] C. Halsband, H. Kurihara, Potential acidification impacts on zooplankton in CCS leakage scenarios, Mar Pollut Bull. 73 (2013) 495–503, https://doi.org/10.1016/j.marpolbul.2013.03.013.
[3] C. Ma, B. Scott, G. Pickrell, A. Wang, Porous capillary tubing waveguide for multigas sensing, Opt Lett, OL. 35 (2010) 315–317, https://doi.org/10.1364/OL.35.000315.
[4] C. Gouveia, A. Markovics, J. Baptista, B. Kovacs, P. Jorge, Measurement of CO2 using refractometric fiber optic sensors, in: Proc. 3rd WSEAS Int Conf Adv Sensors, 2010: pp. 169–173.
[5] L. Melo, G. Burton, B. Davies, D. Risk, P. Wild, Highly sensitive coated long period grating sensor for CO2 detection at atmospheric pressure, Sensors Actuator B: Chem. 202 (2014) 294–300, https://doi.org/10.1016/j.snb.2014.05.062.
[6] G. Mi, C. Horvath, M. Aktary, V. Van, Silicon microring refractometric sensor for atmospheric CO_2 gas monitoring, Opt Express, OE. 24 (2016) 1773–1780, https://doi.org/10.1364/OE.24.001773.
[7] M.G. Allen, K.L. Carleton, S.J. Davis, W.J. Kessler, C.E. Otis, D.A. Palombo, D.M. Sonnenfroh, Ultrasensitive dual-beam absorption and gain spectroscopy: applications for near-infrared and visible diode laser sensors, Appl Op., AO. 34 (1995) 3240–3249, https://doi.org/10.1364/AO.34.003240.
[8] R.P. Lippmann, Pattern classification using neural networks, IEEE Commun Mag. 27 (1989) 47–50, https://doi.org/10.1109/35.41401.
[9] A. Fomin, T. Zavlev, I. Rahinov, S. Cheskis, A fiber laser intracavity absorption spectroscopy (FLICAS) sensor for simultaneous measurement of CO and CO2 concentrations and temperature, Sensors Actuator B: Chem. 210 (2015) 431–438, https://doi.org/10.1016/j.snb.2015.01.001.
[10] W. Ma, R. Wang, Q. Rong, Z. Shao, W. Zhang, T. Guo, J. Wang, X. Qiao, CO2 gas sensing using optical fiber Fabry–Perot interferometer based on Polyethyleneimine/Poly(vinyl alcohol) coating, IEEE Photonics J. 9 (2017) 1–8, https://doi.org/10.1109/JPHOT.2017.2700053.
[11] R. Wang, X. Qiao, Hybrid optical fiber Fabry–Perot interferometer for simultaneous measurement of gas refractive index and temperature, Appl Opt. 53 (2014) 7724–7728, https://doi.org/10.1364/AO.53.007724.
[12] R. Wang, X. Qiao, Gas refractometer based on optical fiber extrinsic Fabry—Perot interferometer with open cavity, IEEE Photon Technol Lett. 27 (2015) 245–248, https://doi.org/10.1109/LPT.2014.2365812.
[13] B.N. Shivananju, S. Yamdagni, R. Fazuldeen, A.K. Sarin Kumar, G.M. Hegde, M.M. Varma, S. Asokan, CO2 sensing at room temperature using carbon nanotubes coated core fiber Bragg grating, Rev Sci Instrum. 84 (2013), 065002, https://doi.org/10.1063/1.4810016.
[14] T.C.D. Doan, J. Baggerman, R. Ramaneti, H.D. Tong, A.T.M. Marcelis, C.J.M. van Rijn, Carbon dioxide detection with polyethylenimine blended with polyelectrolytes, Sensor Actuator B Chem. 201 (2014) 452–459, https://doi.org/10.1016/j.snb.2014.05.023.
[15] Md Islam, M. Ali, M.-H. Lai, K.-S. Lim, H. Ahmad, Chronology of Fabry-Perot interferometer fiber-optic sensors and their applications: a review, Sensors. 14 (2014) 7451–7488, https://doi.org/10.3390/s140407451.
[16] D. Jáuregui-Vázquez, J. Estudillo-Ayala, R. Rojas-Laguna, E. Vargas-Rodríguez, J. Sierra-Hernández, J. Hernández-García, R. Mata-Chávez, An all fiber intrinsic Fabry-Perot interferometer based on an air-microcavity, Sensors. 13 (2013) 6355–6364, https://doi.org/10.3390/s130506355.
[17] S. Pevec, D. Donlagic, Miniature fiber-optic Fabry-Perot refractive index sensor for gas sensing with a resolution of $5x10^{-9}$ RIU, Opt Express. 26 (2018), 23868, https://doi.org/10.1364/OE.26.023868.
[18] J. Luo, S. Liu, P. Chen, S. Lu, Q. Zhang, Y. Chen, B. Du, J. Tang, J. He, C. Liao, Y. Wang, Fiber optic hydrogen sensor based on a Fabry–Perot interferometer with a fiber Bragg grating and a nanofilm, Lab Chip. 21 (2021) 1752–1758, https://doi.org/10.1039/D1LC00012H.
[19] N.L. Kazanskiy, M.A. Butt, S.N. Khonina, Carbon dioxide gas sensor based on Polyhexamethylene Biguanide polymer deposited on silicon nano-cylinders metasurface, Sensors. 21 (2021) 378, https://doi.org/10.3390/s21020378.
[20] J. Peng, W. Feng, X. Yang, G. Huang, S. Liu, Dual Fabry–Pérot interferometric carbon monoxide sensor based on the PANI/Co_3O_4 sensitive membrane-coated Fibre tip, Z Naturforsch. 74 (2019) 101–107, https://doi.org/10.1515/zna-2018-0453.
[21] F. Zhang, N. Zhao, Q. Lin, Z. Wu, B. Tian, P. Shi, P. Yang, Z. Jiang, The influence of key characteristic parameters on performance of optical fiber Fabry–Perot temperature sensor, AIP Adv. 10 (2020), 085118, https://doi.org/10.1063/5.0005151.
[22] M. Njegovec, D. Donlagic, A fiber-optic gas sensor and method for the measurement of refractive index dispersion in NIR, Sensors. 20 (2020) 3717, https://doi.org/10.3390/s20133717.
[23] S. Sivasubramanian, A. Widom, Y.N. Srivastava, The Clausius–Mossotti phase transition in polar liquids, Phys Stat Mech Appl. 345 (2005) 356–366, https://doi.org/10.1016/j.physa.2004.05.088.
[24] M.E. Edwards, Y.H. Hwang, X. Wu, Large deviations from the Clausius-Mossotti equation in a model microemulsion, Phys Rev E. 49 (1994) 4263–4267, https://doi.org/10.1103/PhysRevE.49.4263.